Expression of GPR177 (Wntless/Evi/Sprinter), a Highly Conserved Wnt-Transport Protein, in Rat Tissues, Zebrafish Embryos, and Cultured Human Cells

Jay Jin, **Megan Morse**, **Colleen Frey**, **Jessica Petko**, and **Robert Levenson**[*]
Department of Pharmacology, Pennsylvania State College of Medicine, Hershey, PA 17033

Abstract

GPR177 is an evolutionarily conserved transmembrane protein necessary for Wnt protein secretion. Little is currently known, however, regarding expression of GPR177, especially in vertebrate species. We have developed an antiserum against GPR177, and used it to examine expression of GPR177 in human tissue culture cells, adult mouse and rat tissues, as well as developing zebrafish embryos. In rodents, GPR177 is expressed in virtually all tissue types and brain regions examined. In zebrafish, GPR177 polypeptides are expressed throughout embryogenesis, and are detectable as early as one hour post-fertilization. *In situ* hybridization analysis reveals that *gpr*177 mRNA expression is prominent in embryonic zebrafish brain and ear. Structural studies suggest that GPR177 is modified by N-linked sugars, and that the protein contains an even number of transmembrane segments. The relatively ubiquitous expression of GPR177 suggests that this protein may serve to regulate Wnt secretion in a variety of embryonic and adult tissue types.

Keywords

GPR177; wntless; zebrafish; rodents; expression; structure/function

INTRODUCTION

Wnts are a family of secreted glycoproteins that regulate cellular interactions in the surrounding tissue. In metazoans, Wnt proteins mediate many developmental processes during embryogenesis including anterior-posterior axis formation, cell polarity, and cell migration (Wodarz and Nusse, 1998; Logan and Nusse, 2004). In adult organisms, Wnt proteins have been shown to help maintain stem cell populations (Reya et al., 2003; Willert et al., 2003; Reya and Clevers, 2005), while aberrant regulation of Wnts and their signal-transduction cascades have been linked to the formation of various human cancers (Clevers, 2006; Klaus and Birchmeier, 2008). Though many of the downstream effects and effectors of Wnt signaling have been elucidated, much less is known about the molecular mechanisms that contribute to the maturation of Wnt proteins and their secretion from Wnt-producing cells.

Recently, a novel Wnt pathway component was identified in *Drosophila* called *wntless* (*wls*) (Banziger et al., 2006), *evenness interrupted* (*evi*) (Bartscherer et al., 2006), or *sprinter* (*srt*) (Goodman et al., 2006). *Wls/evi/srt* encodes a multipass transmembrane protein that is highly conserved in metazoans from worms to humans. Wntless/Evi/Sprinter is specifically

[*]Corresponding Author Department of Pharmacology, Penn State College of Medicine Hershey, PA 17033 Phone: (717) 531-4545 FAX: (717) 531-5013 rlevenson@hmc.psu.edu.

required for Wnt secretion in *Drosophila*, and localizes to components of the secretory pathway including Golgi, endosomes, and the plasma membrane (Banziger et al., 2006; Belenkaya et al., 2008; Franch-Marro et al., 2008; Yang et al., 2008). The mammalian ortholog of Wntless/Evi/Sprinter is GPR177, a putative orphan G-protein coupled receptor (GPCR) (Fu et al., 2009). While GPR177 has been shown to regulate Wnt protein secretion in mammalian cells (Banziger et al., 2006; Bartscherer et al., 2006; Belenkaya et al., 2008; Franch-Marro et al., 2008; Port et al., 2008), it is not known whether GPR177 may also function as a GPCR. The number and location of the transmembrane segments in GPR177 is also controversial, with models predicting either four (Goodman et al., 2006), seven (Banziger et al., 2006), or eight (Bartscherer et al., 2006) membrane spanning domains. In murine cell lines, GPR177 appears to mediate Wnt protein secretion, while in mice, gene knockout experiments strongly suggest that GPR177 is essential for viability, as homozygous null mutants die *in utero* prior to day E10.5 (Fu et al., 2009).

Sequence comparisons indicate that GPR177 is extremely highly conserved between vertebrate species. For example, human GPR177 is 96% identical to mouse GPR177 and 78% identical to the zebrafish protein. Based on this high degree of sequence similarity, it seems reasonable to assume that the general function of GPR177, namely regulation of Wnt protein secretion, is also likely to be conserved across species lines. This idea is supported by experiments that demonstrate that human GPR177 is also required for Wnt secretion (Banziger et al., 2006; Bartscherer et al., 2006; Belenkaya et al., 2008; Franch-Marro et al., 2008; Port et al., 2008). These reports suggest that while the overall function of GPR177 is the same, there may be species and cell-type specific mechanisms of Wnt release involving GPR177. Thus, it will be important to determine the specific expression profile of GPR177 in developing and adult organisms. In this report, we examine GPR177 expression during zebrafish embryogenesis and in adult mouse and rat tissues in an effort to better understand the significance of this protein's role in Wnt secretion in vertebrate organisms.

RESULTS

GPR177 Antibodies are Specific for GPR177 and Immunoreactive Across Species

To analyze GPR177 expression, anti-GPR177 antibodies were raised against a peptide antigen corresponding to the C-terminal 18 amino acids of human GPR177. The specificity of the anti-GPR177 antisera was analyzed by transfecting HEK 293 cells with either FLAG/ 6× His-tagged GPR177 or untagged GPR177 cDNAs. A Western blot containing lysates prepared from transfected cells was first probed with anti-GPR177 antibodies (Fig. 1A, left panel). A single band of ~46 kDa was detected in lysates prepared from cells expressing untagged GPR177 (GPR177 lane), whereas two bands of ~46 kDa and ~50 kDa were detected in lysates prepared from cells expressing epitope-tagged GPR177 (FLAG-HIS lane). The 46 kDa band migrates at the same position as the untagged GPR177 polypeptide, and represents GPR177 endogenously expressed in HEK 293 cells, while the 50 kDa band represents the epitope-tagged GPR177 polypeptide. The mobility difference between the 46 and 50 kDa GPR177 bands corresponds to the size of the FLAG/6× His tag. When the blot was stripped and reprobed with anti-FLAG antibodies, a single band migrating at the position of epitope-tagged GPR177 (~50 kDa) was detected in the FLAG-HIS lane, but not in the untagged GPR177 lane (Fig. 1A, right panel). Taken together, these results provide strong evidence that the anti-GPR177 antibodies react specifically with GPR177.

Sequence comparisons indicate that the C-terminal peptide used to generate anti-GPR177 antibodies is very highly conserved. This segment of human, mouse, and rat GPR177 are 100% identical, while the human and zebrafish proteins differ at only 2 of 18 residues in this domain. Based on this high degree of sequence conservation, we asked whether the anti-human GPR177 antibodies would immunoreact with GPR177 from a variety of species. A

Western blot containing lysates prepared from two human cell lines (HEK 293 and SH-SY5Y), and rat, mouse, and zebrafish brains was probed with anti-GPR177 antibodies. As shown in Fig. 1B, anti-GPR177 antibodies are reactive with a single polypeptide in each species. We detected an immunoreactive band of ~46 kDa in lysates from both human cell lines (Fig. 1B). This band migrates with a mobility similar to that of untagged GPR177 (Fig. 1A). A band migrating at ~46 kDa was detected in mouse brain lysates, while a slightly larger band of ~49 kDa was detected in rat brain lysates. In contrast, zebrafish GPR177 appears somewhat smaller, migrating with an apparent molecular weight of ~43 kDa. These results indicate that anti-human GPR177 antibodies immunoreact with endogenous GPR177 from a variety of vertebrate species. It is possible that the mobility differences in GPR177 seen on immunoblots may reflect species- or tissue-specific differences in post-translational modifications.

Expression of GPR177 in Rodent Tissues and Brain Regions

Having established the specificity of the anti-GPR177 antibodies, we analyzed expression of GPR177 in a variety of rat and mouse tissues. As shown in Fig. 2A, GPR177 was expressed in all rat tissues tested including skeletal muscle, heart muscle, lung, gut, liver, and kidney. The slight differences in mobility of GPR177 on SDS-PAGE from tissue to tissue, may reflect differences in post-translational modifications. GPR177 polypeptides were also detected in all mouse tissues examined (Fig. 2B). In mouse, GPR177 migrates with an apparent molecular weight of ~46 kDa in each of the five tissues tested.

We have previously shown that GPR177 interacts with the mu-opioid receptor (MOR) to regulate Wnt protein secretion (Jin et al., 2010). We were therefore interested in examining the distribution of GPR177 in various brain regions. To perform this analysis, we probed lysates prepared from several rat and mouse brain regions including cortex, striatum, hippocampus (rat and mouse), ventral tegmentum, nucleus accumbens (rat), and cerebellum (mouse). As shown in Fig. 2C and D, GPR177 is expressed at similar levels in all brain regions tested (both rat and mouse) with the possible exception of hippocampus, where GPR177 is present at somewhat lower abundance. In cerebellum, expression of mouse GPR177 mRNA (Fig. 2E) and rat GPR177 protein (Fig. 2F–H) was localized predominantly within Purkinje cells. This distribution appears comparable in mouse and rat cerebellum.

Expression of the Zebrafish *gpr177* Gene During Zebrafish Embryogenesis

Western blot analysis and whole mount *in situ* hybridization were used to examine the spatio-temporal expression of the single zebrafish *gpr177* gene during early embryonic development. As shown in Fig. 3J, GPR177 polypeptides were expressed at similar levels during the first ten hours of zebrafish embryonic development. GPR177 polypeptides were present at all stages of embryogenesis through 72 hours post-fertilization (hpf; data not shown).

Expression of *gpr177* mRNA is shown in Fig. 3A–I. At early somitogenesis (15 hpf), mRNA transcripts were detected in the presumptive head and tailbud (Fig. 3A), and in the head region, spinal cord, and tail bud at 18 hpf (Fig. 3B). Expression of the *gpr177* gene persisted in the spinal cord at 24 hpf, and was also detected in the midbrain, hindbrain, midbrain-hindbrain boundary, and ventricular zone (Fig. 3C). At 48 hpf, transcripts of the *gpr177* gene were predominant in the tectum, branchial arches, pectoral fin bud, hindbrain, midbrain-hindbrain boundary, ventricular zone, and ear (Fig. 3D–F). By 72 hpf, *gpr177* mRNA expression was restricted primarily to the branchial arches, midbrain-hindbrain boundary, ventricular zone, and the semicircular canals of the inner ear (Fig. 3G–I).

To analyze the embryonic function of the *gpr177* gene, we used two, non-overlapping antisense morpholinos to knock down *gpr177* mRNA translation in developing zebrafish. One MO was generated to target the initiating methionine (ATG-MO), while the other was made to target a portion of the upstream 5'-untranslated region (UTR-MO) of zebrafish *gpr177* mRNA. Injection of either MO into one-cell stage embryos produced noticeable effects on brain and ear development (Fig. 4), whereas embryos injected with Danieau buffer alone showed no obvious defects. At 24 hpf, morphant embryos (Fig. 4C, D) exhibited a slightly diminished head size and smaller otic vesicle compared with wild-type embryos (Fig. 4A, B). The most noticeable defect in 24 hpf morphants was the extensive disorganization of brain tissue and poorly defined midbrain-hindbrain boundary. At 48 hpf, the eyes of morphant embryos (Fig. 4G, H, J, K) appeared somewhat smaller compared to wild-type embryos (Fig. 4E, F), and brain tissue remained disorganized, with the absence of a clearly identifiable midbrain-hindbrain boundary (Fig. 4H, K). Morphants at 24 and 48 hpf also exhibited abnormal ventral (Fig. 4J) and lateral (Fig. 4G) curvature of the tail, which resembled phenotypes reported after morpholino-knockdown of zebrafish *wnt3a* and *wnt8* mRNAs (Shimizu et al., 2005). Injection of the ATG-MO produced significant cardiac edema in some embryos (Fig. 4H). This non-specific effect was not observed with the *gpr177* UTR-MO (Fig. 4K). Additionally, knockdown of the *gpr177* gene produced a noticeable effect on ear development in zebrafish embryos. At 48 hpf, wild type otic vesicles contained two characteristic rounded otoliths and displayed formation of the epithelial protrusions of the semicircular canals (Fig. 4F). In morphant embryos at 24 hpf (Fig. 4D) and 48 hpf (Fig. 4H, K), otolith formation appeared normal. At 48 hpf, however, the semicircular canal protrusions were completely absent in morphant embryos (Fig. 4H, K). These results suggest that *gpr177* gene expression is required for proper brain and ear development during zebrafish embryogenesis.

Using the *gpr177* UTR-MO, we analyzed the most prominent morphant phenotypes that were produced over a range of morphlino doses. By 48 hpf, the number of fish that failed to develop semicircular canals and exhibited abnormally curved tails increased in a dose-dependent fashion (Fig. 4L). At the highest dose of UTR-MO (10 ng), nearly 70% of injected embryos developed an abnormally curved tail, whereas semicircular canals failed to develop in 65% of embryos (Fig. 4L). The efficacy of the UTR-MO was confirmed by Western blot analysis of injected embryos. At 48 hpf, the UTR-MO knocked down GPR177 protein levels in a dose-dependent fashion. At the highest dose of MO used (10 ng), GPR177 expression was reduced by ~60% (Fig. 4M).

GPR177 Structure-Function Relationships

Sequence analysis of sprinter, the *Drosophila* ortholog of vertebrate GPR177, predicts two potential N-linked glycosylation sites within the first extracellular domain of the protein (Goodman et al., 2006). Using the NetNGlyc 1.0 server (http://www.cbs.dtu.dk/services/NetNGlyc/), we identified two potential N-linked glycosylation sites in the human GPR177 sequence at residues N8 and N406. To determine the glycosylation state of GPR177, we treated microsomes from GPR177-transfected HEK 293 cells with *N*-glycosidase F. Microsomes from rat and mouse brain, which endogenously express GPR177, were also digested with the enzyme. As shown in Fig. 5A, *N*-glycosidase F digestion of either HEK 293 cell (left panel), rat brain (middle panel), or mouse brain (right panel) microsomes produced a novel polypeptide migrating with an apparent molecular mass of ~37 (human) or ~34 kDa (rat and mouse). The difference in mobility between the human and rodent GPR177 core protein reflects the presence of the FLAG/6× His epitope tag on the human protein. These results suggest that the human and rodent GPR177 polypeptides are modified by the addition of N-linked oligosaccharides.

Secondary structure analyses predict that GPR177 may contain as many as four, seven or eight membrane spanning domains, as well as a putative N-terminal signal sequence (Banziger et al., 2006; Bartscherer et al., 2006; Goodman et al., 2006). However, when we transfected GPR177 cDNAs containing an N-terminal FLAG/6x His-tag into HEK 293 cells, we were able to detect expression of the constructs on immunoblots with anti-FLAG antibodies (Figs. 1A, 5A), suggesting that the putative signal sequence was not cleaved from the GPR177 polypeptide.

Models in which the N-terminus of GPR177 is either external (Banziger et al., 2006) or internal (Goodman et al., 2006) have been proposed. We utilized the FLAG/6× His-tagged GPR177 construct to analyze whether the GPR177 N-terminus is displayed intracellularly or extracellularly. HEK 293 cells were transfected with the N-terminal FLAG/6× His-tagged GPR177 construct and the distribution of the tagged protein was analyzed by immunofluorescence microscopy. Cells transfected with an N-terminal FLAG-tagged MOR cDNA served as controls. The results are shown in Fig. 5. Under permeabilized conditions, HEK 293 cells transfected with the N-terminal FLAG-tagged MOR cDNA exhibited robust staining at the plasma membrane and a punctate pattern throughout the cytoplasm (Fig. 5B). Cells expressing the FLAG/6× His-tagged GPR177 construct showed punctate cytoplasmic staining as well as staining at the plasma membrane (Fig. 5D). The transfection efficiency and protein expression levels of the two constructs were virtually identical (data not shown). In non-permeabilized cells, the tagged MOR construct was visualized at the cell surface (Fig. 5A). However, virtually no immunostaining was detectablein non-permeabilized cells transfected with the N-terminal tagged GPR177 cDNA (Fig. 5C). These results strongly suggest that the N-terminus of GPR177 is located intracellularly, and that the protein is likely to contain an even number of transmembrane segments.

To determine whether epitope-tagged GPR177 is in fact functional, we asked whether the FLAG/6× His-tagged GPR177 cDNA could support Wnt protein secretion in our Wnt secretion assay. As shown in Fig. 5F, our data indicate that in transfected HEK 293 cells, both untagged and FLAG/6× His-tagged GPR177 cDNAs are capable of supporting Wnt3 secretion. Cotransfection of myc-tagged Wnt3 (Wnt3-myc) and untagged GPR177 cDNAs produced a 5-fold increase in Wnt3 protein secretion compared to cotransfection of Wnt3-myc plus an empty expression vector. Cotransfection of Wnt3-myc and FLAG/6× His-tagged GPR177 cDNA resulted in a 7-fold increase Wnt3 protein secretion compared to the control (Fig. 5F). Taken together, these results demonstrate that the N-terminus of GPR177 does not appear to constitute a cleavable signal sequence, and that the presence of this domain on the mature protein does not appear to interfere with the ability of GPR177 to support Wnt protein secretion.

DISCUSSION

We have developed an antiserum against the conserved C-terminus of (human) GPR177, and used this antiserum to examine GPR177 protein expression and structure/function relationships. The antiserum is extremely clean, and on Western blots recognizes a single polypeptide in lysates from human fibroblast and neuroblastoma cell lines. The antisera is also reactive with GPR177 polypeptides present in rats, mice, and zebrafish. In adult rats and mice, GPR177 was ubiquitously expressed in all tissue types examined. GPR177 polypeptide expression was also detected in embryonic and adult zebrafish. Sequence analysis predicts the possibility for a second isoform of GPR177 derived by alternative mRNA splicing. However, it is unlikely that our anti-GPR177 antisera will detect expression of this novel GPR177 isoform since the predicted polypeptide contains a highly divergent C-terminal domain.

Recent experiments in mice indicate that GPR177 is an essential gene. Mouse embryos with deficient GPR177 expression exhibit defects in anterior-posterior axis formation and die *in utero* prior to day E10.5 (Fu et al., 2009). GPR177 null embryos failed to develop distinct structures but grew instead as egg cylinders. In addition, the mesoderm and primitive streak were missing and the excess ectoderm became irregular and folded (Fu et al., 2009). To gain further insight into the functional role of GPR177 in embryogenesis, we utilized antisense morpholinos (MOs) to knock down translation of GPR177 mRNA in developing zebrafish. An advantage of the morpholino knockdown approach is that it is possible to generate hypomorphs (Cheng et al., 2003). Thus it is possible to produce recognizable phenotypes without inducing lethality in early embryogenesis, as occurs when GPR177 is knocked out in mice (Fu et al., 2009). We found that microinjection of a GPR177 MO into one cell-stage zebrafish embryos produced a striking effect on brain and inner ear development. At 48 hpf, morphants exhibited severely disorganized brain tissue, absence of a clear midbrain-hindbrain boundary, loss of semicircular canal formation, and abnormal curvature of the tail. These phenotypes are consistent with the major expression sites we observed for GPR177 mRNA transcripts. Besides displaying significant cardiac edema and mild developmental delay, two common non-specific side effects produced by MO injections, morphant embryos exhibited no obvious gross defects. Thus, we conclude that in zebrafish embryos, GPR177 is required for proper development of the central nervous system as well as structural components of the inner ear.

Although the current study was focused primarily on elucidating the spatio-temporal profile of GPR177 expression, we also examined several aspects of GPR177 structure/function. One important, but as yet unresolved issue concerns the number of transmembrane segments contained within the mature GPR177 polypeptide. Models in which GPR177 contains four (Goodman et al., 2006), seven (Banziger et al., 2006) or eight (Bartscherer et al., 2006) membrane spanning domains have all been proposed. Each model also predicts that GPR177 contains an N-terminal signal sequence. Determining which of these diverse models is correct is of some interest, since virtually all data banks classify GPR177 as an orphan seven transmembrane GPCR (Ota et al., 2004). By transfecting GPR177 cDNA containing an N-terminal epitope tag into HEK 293 cells, we were able to detect expression of the tagged protein on Western blots, suggesting that the putative signal sequence was in fact not cleaved. The presence of the epitope tag did not appear to impede GPR177 function, since the tagged protein was capable of supporting Wnt protein secretion in an *in vitro* assay. Cellular localization studies of GPR177 carrying an N-terminal tag also demonstrate that the N-terminus of the protein is likely to be located within the cytosol. Previous studies have shown that the C-terminus of GPR177 is also located intracellularly (Korkut et al., 2009). It is therefore highly likely that GPR177 possesses an even number of transmembrane segments. Since GPR177 does not appear to exhibit the seven transmembrane structure characteristic of most GPCRs, our results do not support the view that GPR177 represents an orphan GPCR.

Determining the exact number and locations of the transmembrane segments within GPR177 will also be of relevance to elucidating the sites of N-linked glycosylation within the polypeptide. We identified two potential N-linked glycosylation sites in the human GPR177 sequence at residues N8 and N406 using the NetNGlyc algorithm. Based on our finding that the N-terminus of GPR177 is likely to be intracellular, residue N8 is predicted to be located in the cytosol which would preclude it from being glycosylated. Similarly, residue N406 is predicted to be located cytoplasmically in all three models of GPR177 structure, and therefore is also not likely to be glycosylated. An asparagine residue, located at position N69, could also serve as a site for N-linked glycosylation. Although this site is predicted to be extracellular in all three models of GPR177 structure, mutation of N69 to threonine did alter the mobility of the mutated protein on SDS-PAGE, suggesting that N69 is not

glycosylated (data not shown). There are an additional 12 potential extracellular asparagine residues in human GPR177. Determining which of these asparagine residues may be modified by N-linked oligosaccharides will be relevant to elucidating the membrane topology of GPR177. In this context, it is of interest to note that after digestion with *N*-glycosidase F, the endogenous GPR177 core protein migrates on SDS-PAGE with an apparent molecular mass of ~34 kDa. This is somewhat smaller than the molecular mass of ~46 kDa for the GPR177 polypeptide predicted by protein sequence algorithms. Further structural studies will be needed to clarify the reason that the GPR177 core protein appears to run anomalously on SDS-PAGE.

The ubiquitous expression of GPR177 in rodent tissues suggests that GPR177 plays a role in regulating Wnt secretion in a diverse range of tissue types. In the future, it will be important to further define the expression of GPR177 at the cellular level. It may be of interest, for example, to know whether GPR177 is expressed in cell types that do not express or secrete Wnt proteins. The expression of GPR177 in non-Wnt producing cells would hint at the possibility that GPR177 may play a role in cellular functions beyond its role in Wnt secretion.

EXPERIMENTAL PROCEDURES

Cell culture and transfection

Human Embryonic Kidney (HEK) 293 cells were maintained in Dulbecco's Modified Eagle's Medium (DMEM) supplemented with 10% fetal bovine serum (FBS). SH-SY5Y (ATCC, Manassas, VA) human neuroblastoma cells were maintained in DMEM supplemented with 10% FBS. Transfections of HEK 293 cells were carried out using Effectene transfection reagent (Qiagen, Valencia, CA) according to manufacturer's instructions.

Animals and tissue isolation

All animals were maintained and sacrificed according the guidelines set forth by the Penn State College of Medicine IACUC. Tissues were harvested from adult Sprague-Dawley rats and an adult BL/6 mouse, frozen on dry ice, and thawed prior to homogenization in lysis buffer (Hannan et al., 2008). Brain regions were dissected and lysates prepared immediately after animals were sacrificed.

Antibody production and immunohistochemistry

Anti-GPR177 antibodies were raised in chickens (Gene-Tel Laboratories, Madison, WI) against a peptide antigen corresponding to the C-terminal 18 amino acids (HVDGPTEIYKLTRKEAQE) of human GPR177. Chicken polyclonal antibodies of the IgY subtype were harvested from egg yolks and affinity-purified prior to use.

Fresh frozen brains from adult Sprague-Dawley rats were saggitally sectioned (16 μm thick slices), fixed in 4% formaldehyde, washed with phosphate-buffered saline (PBS), then blocked in 10% goat serum, 0.1% Triton X-100, 0.1 M PBS, pH 7.4. Sections were incubated with anti-GPR177 antibodies (1:500 dilution) and immunoreactivity detected using Cy3-conjugated goat anti-chicken secondary antibodies (1:5000 dilution; Jackson ImmunoResearch, West Grove, PA). Confocal images were captured on a Leica TCS SP2 AOBS microscope using either 20× or 63× objectives.

Immunocytochemistry

HEK 293 cells were grown on collagen type I coated glass coverslips (BD Biosciences, San Jose, CA) in DMEM supplemented with 10% FBS. Cells were transiently transfected with

FLAG/6× His-tagged GPR177 or FLAG-tagged mu-opioid receptor (MOR) cDNAs as described above. Transfected cells were examined 24 hours after transfection. Localization of the epitope tag was performed by immunofluorescence microscopy as previously described (Canfield and Levenson, 1993; Canfield et al., 1996). Briefly, non-permeabilized cells were incubated with rabbit anti-FLAG polyclonal antibody (1:250 dilution; Sigma, St. Louis, MO) in DMEM for 1 hour at 4°C. The cells were then fixed in 4% paraformaldehyde and incubated in blocking buffer (0.1 M PBS, 5% goat serum, 1% bovine serum albumin, 0.01% Triton X-100) for 15 minutes prior to incubating with DyLight 594-conjugated goat anti-rabbit secondary antibody (1:500 dilution, Jackson ImmunoResearch). Cells were washed in 0.1 M PBS and mounted on glass slides using ProLong Gold reagent (Invitrogen, Carlsbad, CA). For permeabilized cell staining, cells were chilled on ice for 20 minutes, fixed in 4% paraformaldehyde, then incubated with rabbit anti-FLAG polyclonal antibody (1:500 dilution, Sigma). Cells were incubated with DyLight 594-conjugated goat anti-rabbit secondary antibody (1:500 dilution), then mounted on glass slides using the ProLong Gold reagent. Immunofluoresence images were captured on a Nikon inverted microscope using a 20× objective.

Tissue preparation and immunoblotting

Crude membrane fractions from transfected HEK 293 cells or rat brain lysates were prepared as previously described (Karpa et al., 1999). To deglycosylate GPR177, microsomes were digested with *N*-glycosidase F (PNGaseF; New England BioLabs, Ipswich, MA) according to manufacturer's instructions. Samples were digested with 1.0 unit of PNGaseF for 1 hour at 37°C as described (Karpa et al., 1999). Solubilized membrane fractions were separated on SDS-containing 10% polyacrylamide gels, then transferred to polyvinylidine difluoride (PVDF) membranes. Filters were blocked for 2 hours in Tris-buffered saline with Tween-20 (TBS-T; 20 mM Tris (pH 7.4), 275 mM NaCl, 3 mM KCl, 1% Tween-20) containing 10% dry milk. Blots were incubated with chicken anti-GPR177 antibodies (1:5000 – 1:2500 dilution) for 1 hour, then horseradish-peroxidase (HRP)-conjugated donkey anti-chicken secondary antibodies (1:15:000) for 1 hour. Immunoreactivity was detected using an Enhanced Chemiluminescence (ECL) Plus kit (GE Healthcare, Piscataway, NJ).

Wnt secretion assay

HEK 293 cells were cotransfected with myc-tagged human Wnt3 and FLAG/6× His-tagged GPR177 cDNAs engineered in pCMV-Tag2 (GPR177) or Tag3 (Wnt3) mammalian expression vectors (Stratagene, La Jolla, CA). Cells were grown in DMEM supplemented with 10% FBS for 24 hours, then DMEM alone for an additional 24 hours prior to initiating secretion assays. To assess secretion, medium was collected and concentrated (approximately 22-fold) using an Amicon Ultra-15 centrifugal filter (Millipore, Bedford, MA). Aliquots of medium (45 μl) were fractionated on SDS-containing 10% polyacrylamide gels. Proteins were transferred to a PVDF membrane, and the filter probed with a monoclonal anti-myc antibody (1:2500 dilution, Millipore). Proteins were visualized using HRP-conjugated rabbit anti-mouse secondary antibodies (1:15,000 dilution, Jackson ImmunoResearch). Immunoreactivity was detected using an ECL Plus kit, and scanned blots quantitated using the ImageJ software package (NIH). Data were subjected to a two-tailed Student's t-test.

Zebrafish mRNA and protein expression

The complete open reading frame of zebrafish *gpr177* (GenBank accession no. NM_213146) was generated by RT-PCR from 24 hours post-fertilization (hpf) RNA and used to produce a digoxin-labeled riboprobe. Zebrafish embryos were preserved in 4% paraformaldehyde in PBS. Whole-mount *in situ* hybridization was performed as previously

described (Thisse and Thisse, 2008; Petko et al., 2009). Two non-overlapping antisense morpholino (MO) oligonucleotides directed against the initiating methionine (ATG-MO; 5'-CTCAATAATTGCCCCAGCCATTTTC-3') and 5'-untranslated region (UTR-MO; 5'-AAAGTGCGTCTTCAGACAGGATTGA-3') of *gpr177* mRNA (Gene Tools, Philomath, OR) were generated and used separately to block *gpr177* mRNA translation. Each MO was resuspended in 1× Danieau buffer (58 mM NaCl, 0.7 mM KCl, 0.4 mM MgSO4, 0.6 mM Ca(NO3)$_2$, 5 mM HEPES, pH 7.6), and injected into single cell embryos as previously described (Blasiole et al., 2005; Petko et al., 2009). Morphant embryos were harvested at 48 hpf, homogenized in lysis buffer (Hannan et al., 2008), and analyzed by immunoblotting for GPR177 expression as described above.

For protein expression studies, 40–50 embryos were collected every hour from 1–10 hpf. At each time point, embryos were dechorionated, homogenized in lysis buffer, and solubilized proteins were analyzed by immunoblotting for GPR177 expression as described above.

Acknowledgments

REFERENCES

Banziger C, Soldini D, Schutt C, Zipperlen P, Hausmann G, Basler K. Wntless, a conserved membrane protein dedicated to the secretion of Wnt proteins from signaling cells. Cell. 2006; 125:509–522. [PubMed: 16678095]

Bartscherer K, Pelte N, Ingelfinger D, Boutros M. Secretion of Wnt ligands requires Evi, a conserved transmembrane protein. Cell. 2006; 125:523–533. [PubMed: 16678096]

Belenkaya TY, Wu Y, Tang X, Zhou B, Cheng L, Sharma YV, Yan D, Selva EM, Lin X. The retromer complex influences Wnt secretion by recycling wntless from endosomes to the trans-Golgi network. Dev Cell. 2008; 14:120–131. [PubMed: 18160348]

Blasiole B, Kabbani N, Boehmler W, Thisse B, Thisse C, Canfield V, Levenson R. Neuronal calcium sensor-1 gene ncs-1a is essential for semicircular canal formation in zebrafish inner ear. J Neurobiol. 2005; 64:285–297. [PubMed: 15898063]

Canfield VA, Levenson R. Transmembrane organization of the Na,K-ATPase determined by epitope addition. Biochemistry. 1993; 32:13782–13786. [PubMed: 7505614]

Canfield VA, Norbeck L, Levenson R. Localization of cytoplasmic and extracellular domains of Na,K-ATPase by epitope tag insertion. Biochemistry. 1996; 35:14165–14172. [PubMed: 8916902]

Cheng KC, Levenson R, Robishaw JD. Functional genomic dissection of multimeric protein families in zebrafish. Dev Dyn. 2003; 228:555–567. [PubMed: 14579392]

Clevers H. Wnt/beta-catenin signaling in development and disease. Cell. 2006; 127:469–480. [PubMed: 17081971]

Franch-Marro X, Wendler F, Guidato S, Griffith J, Baena-Lopez A, Itasaki N, Maurice MM, Vincent JP. Wingless secretion requires endosome-to-Golgi retrieval of Wntless/Evi/Sprinter by the retromer complex. Nat Cell Biol. 2008; 10:170–177. [PubMed: 18193037]

Fu J, Jiang M, Mirando AJ, Yu HM, Hsu W. Reciprocal regulation of Wnt and Gpr177/mouse Wntless is required for embryonic axis formation. Proc Natl Acad Sci U S A. 2009; 106:18598–18603. [PubMed: 19841259]

Goodman RM, Thombre S, Firtina Z, Gray D, Betts D, Roebuck J, Spana EP, Selva EM. Sprinter: a novel transmembrane protein required for Wg secretion and signaling. Development. 2006; 133:4901–4911. [PubMed: 17108000]

Hannan MA, Kabbani N, Paspalas CD, Levenson R. Interaction with dopamine D2 receptor enhances expression of transient receptor potential channel 1 at the cell surface. Biochim Biophys Acta. 2008; 1778:974–982. [PubMed: 18261457]

Jin J, Kittanakom S, Wong V, Reyes BA, Van Bockstaele EJ, Stagljar I, Berrettini W, Levenson R. Interaction of the mu-opioid receptor with GPR177 (Wntless) inhibits Wnt secretion: potential implications for opioid dependence. BMC Neurosci. 2010; 11:33. [PubMed: 20214800]

Karpa KD, Lidow MS, Pickering MT, Levenson R, Bergson C. N-linked glycosylation is required for plasma membrane localization of D5, but not D1, dopamine receptors in transfected mammalian cells. Mol Pharmacol. 1999; 56:1071–1078. [PubMed: 10531415]

Klaus A, Birchmeier W. Wnt signalling and its impact on development and cancer. Nat Rev Cancer. 2008; 8:387–398. [PubMed: 18432252]

Korkut C, Ataman B, Ramachandran P, Ashley J, Barria R, Gherbesi N, Budnik V. Trans-synaptic transmission of vesicular Wnt signals through Evi/Wntless. Cell. 2009; 139:393–404. [PubMed: 19837038]

Logan CY, Nusse R. The Wnt signaling pathway in development and disease. Annu Rev Cell Dev Biol. 2004; 20:781–810. [PubMed: 15473860]

Ota T, Suzuki Y, Nishikawa T, Otsuki T, Sugiyama T, Irie R, Wakamatsu A, Hayashi K, et al. Complete sequencing and characterization of 21,243 full-length human cDNAs. Nat Genet. 2004; 36:40–45. [PubMed: 14702039]

Petko JA, Kabbani N, Frey C, Woll M, Hickey K, Craig M, Canfield VA, Levenson R. Proteomic and functional analysis of NCS-1 binding proteins reveals novel signaling pathways required for inner ear development in zebrafish. BMC Neurosci. 2009; 10:27. [PubMed: 19320994]

Port F, Kuster M, Herr P, Furger E, Banziger C, Hausmann G, Basler K. Wingless secretion promotes and requires retromer-dependent cycling of Wntless. Nat Cell Biol. 2008; 10:178–185. [PubMed: 18193032]

Reya T, Clevers H. Wnt signalling in stem cells and cancer. Nature. 2005; 434:843–850. [PubMed: 15829953]

Reya T, Duncan AW, Ailles L, Domen J, Scherer DC, Willert K, Hintz L, Nusse R, Weissman IL. A role for Wnt signalling in self-renewal of haematopoietic stem cells. Nature. 2003; 423:409–414. [PubMed: 12717450]

Shimizu T, Bae YK, Muraoka O, Hibi M. Interaction of Wnt and caudal-related genes in zebrafish posterior body formation. Dev Biol. 2005; 279:125–141. [PubMed: 15708563]

Thisse C, Thisse B. High-resolution in situ hybridization to whole-mount zebrafish embryos. Nat Protoc. 2008; 3:59–69. [PubMed: 18193022]

Willert K, Brown JD, Danenberg E, Duncan AW, Weissman IL, Reya T, Yates JR 3rd, Nusse R. Wnt proteins are lipid-modified and can act as stem cell growth factors. Nature. 2003; 423:448–452. [PubMed: 12717451]

Wodarz A, Nusse R. Mechanisms of Wnt signaling in development. Annu Rev Cell Dev Biol. 1998; 14:59–88. [PubMed: 9891778]

Yang PT, Lorenowicz MJ, Silhankova M, Coudreuse DY, Betist MC, Korswagen HC. Wnt signaling requires retromer-dependent recycling of MIG-14/Wntless in Wnt-producing cells. Dev Cell. 2008; 14:140–147. [PubMed: 18160347]
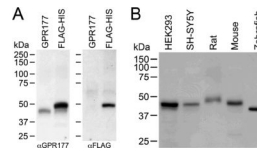
Figure 1. Specificity of anti-GPR177 antibodies
(A) HEK 293 cells were transfected with either untagged GPR177 (GPR177) or N-terminal FLAG/6× His-tagged GPR177 (FLAG-HIS) cDNAs. A Western blot containing lysate from transfected cells was probed with anti-GPR177 antibodies, then stripped and reprobed with anti-FLAG antibodies. **(B)** A Western blot containing lysates prepared from HEK 293 and SH-SY5Y cells, and rat, mouse, and zebrafish brains, was probed with anti-GPR177 antibodies. Molecular weight markers (kDa) are shown at the left.
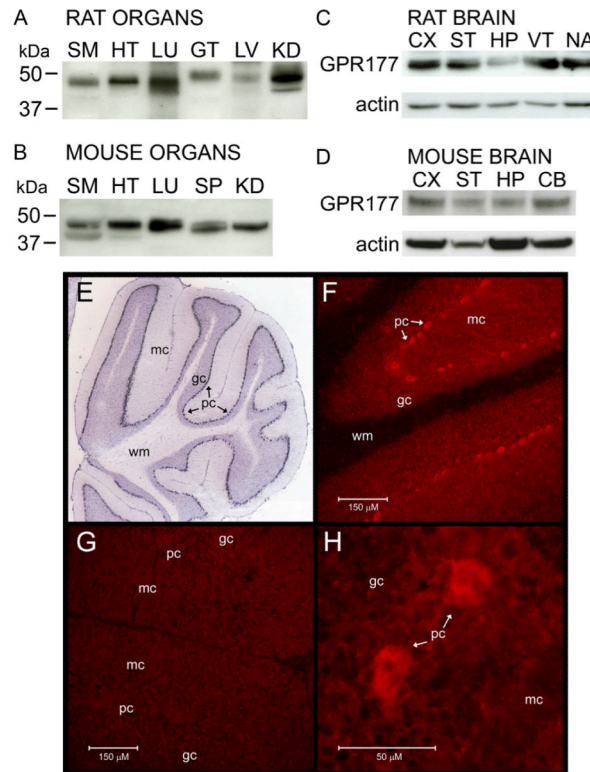
Figure 2. Expression of GPR177 in rat and mouse tissues
Western blots containing lysates from various rat **(A)** and mouse **(B)** tissues were probed with anti-GPR177 antibodies. Western blots containing lysates from various rat **(C)** and mouse **(D)** brain regions were probed with anti-GPR177 antibodies. **(C, D)** Immunoblots were stripped and reprobed with anti-β-actin antibodies. SM: skeletal muscle; HT: heart muscle; LU: lung; GT: gastrointestinal tract; LV: liver; SP: spleen; KD: kidney; CX: cortex; ST: striatum; HP: hippocampus; VT: ventral tegmentum; NA: nucleus accumbens; CB: cerebellum. Molecular weight markers (kDa) are shown at the left. **(E)** *In situ* hybridization of GPR177 mRNA in mouse cerebellum. Image reproduced with permission from Allen Mouse Brain Atlas [Internet]. Seattle (WA): Allen Institute for Brain Science. ©2009. Available from: http://mouse.brain-map.org. Confocal images of rat cerebellum slices stained with anti-GPR177 antibodies **(F, H)**, or no primary antibody **(G)**. Arrows indicate Purkinje cell layer. wm: white matter tract; gc: granular cell layer; pc: purkinje cell layer; mc: molecular layer.
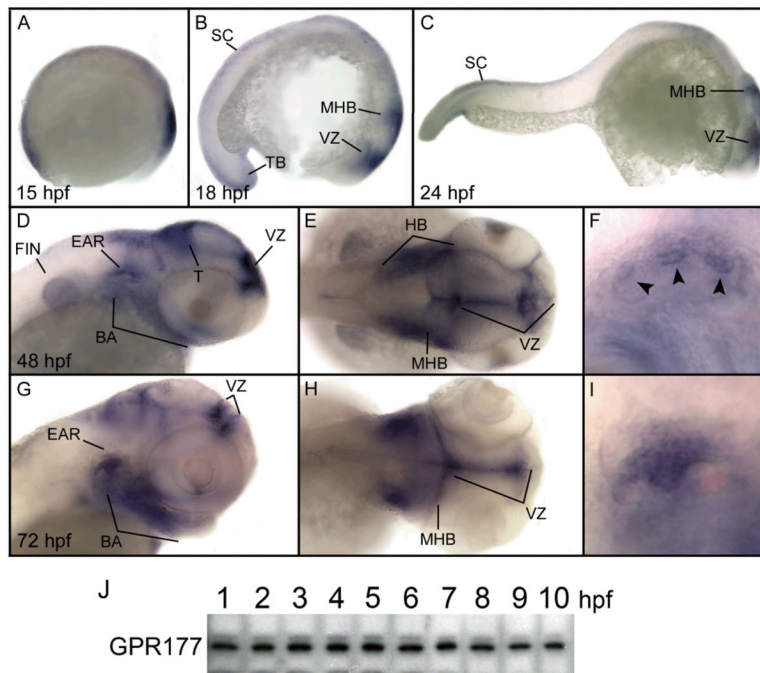
Figure 3. Expression of the *gpr177* gene in zebrafish embryos
Expression of *gpr177* mRNA was analyzed by whole mount *in situ* hybridization **(A–I)**. **(A)** Early somitogenesis, lateral view, **(B)** 18 hpf, lateral view, **(C)** 24 hpf, lateral view. **(D)** 48 hpf, lateral view of head, **(E)** 48 hpf, dorsal view of head **(F)** 48 hpf, lateral view of ear, **(G)** 72 hpf, lateral view of head, **(H)** 72 hpf, dorsal view of head, **(I)** 72 hpf, lateral view of ear. All views are anterior to the right. Arrowheads indicate protrusions of semicircular canals. BA: branchial arches; T: tectum; HB: hindbrain, MHB: midbrain-hindbrain boundary; SC: spinal cord; TB: tail bud; VZ: ventricular zone. **(J)** Western blot containing lysates from embryonic zebrafish between 1 and 10 hpf were probed using anti-GPR177 antibodies. Data are representative of four separate experiments.
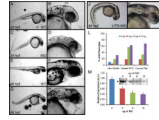
Figure 4. Knockdown of *gpr177* mRNA expression
An antisense *gpr177* MO was used to knock down *gpr177* mRNA translation. All images are lateral views with anterior to the right. Morphants produced by the ATG-MO are in **C**, **D**, **G**, **H**, while morphants produced by the UTR-MO are in **J**, **K**. **(A)** 24 hpf wild type embryo, **(B)** 24 hpf, head of wild type embryo, **(C)** 24 hpf morphant injected with 4 ng of ATG-MO, **(D)** head of 24 hpf morphant, **(E)** 48 hpf wild type embryo, **(F)** head of 48 hpf embryo, **(G)** 48 hpf embryo injected with 4 ng ATG-MO, **(H)** head of 48 hpf morphant, **(J)** 48 hpf embryo injected with 6 ng of UTR-MO, **(K)** head of 48 hpf morphant. Arrows indicate otoliths. Arrowhead indicates protrusions of semicircular canals. MHB: midbrain-hindbrain boundary; OV: otic vesicle; CE: cardiac edema. **(L)** Phenotypes of morphants injected with UTR-MO scored at 48 hpf. n=19–21 at each dose. **(M)** UTR-MO injected embryos (scored in **L**) were harvested at 48 hpf and GPR177 expression compared to that in wild type embryos. Arrowhead indicates position of zebrafish GPR177 (~43 kDa).
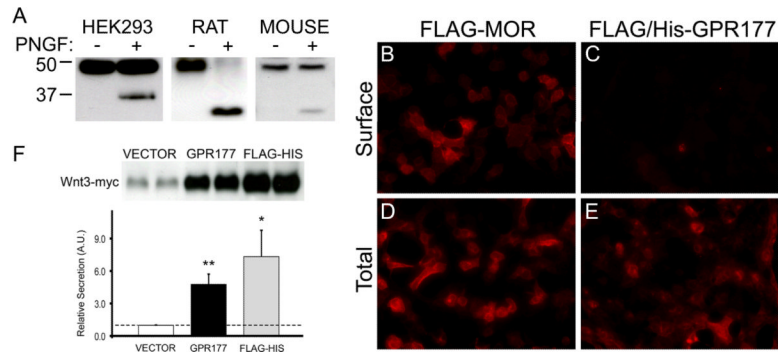
Figure 5. GPR177 structure and function

(A) Crude microsomal membrane preparations from HEK 293 cells transfected with FLAG/ 6× His-tagged GPR177 cDNA (HEK293), rat brain (RAT), and mouse brain (MOUSE) were digested in the presence (+ lanes) or absence (− lanes) of *N*-glycosidase F (PNGF). Lysates were resolved by SDS-PAGE and probed with anti-GPR177 antibodies. Data are representative of three separate experiments. **(B–E)** HEK 293 cells transfected with FLAG-tagged MOR (FLAG-MOR) or N-terminal FLAG/6× His tagged-GPR177 (FLAG/His-GPR177) cDNA and labeled with anti-FLAG antibodies under permeabilized (Total) and non-permeabilized (Surface) conditions. Representative images from two independent experiments are shown. **(F)** HEK 293 cells were cotransfected with myc-tagged Wnt3 cDNA in pCMV-Tag3B vector and either pCMV-Tag2B vector (VECTOR), untagged GPR177 cDNA in pCMV-Sport6 vector (GPR177), or FLAG/6× His-tagged GPR177 in pCMV-Tag2B vector (FLAG-HIS). Wnt3-myc secretion was assayed as described in Experimental Procedures. Western blots were probed with anti-myc antibodies, and bands were quantitated using ImageJ software (NIH). Data was subjected to two-tailed Student's t-test. Dotted line indicates secretion obtained with empty vector control and assigned a relative value of 1.0 (n= 4–6, **p<0.01, *p<0.05).